Lattice modes in the linear chain compound ZrTe5

A A Zwick, Georges Landa, Robert Carles, M.A. A Renucci, A A Kjekshus

Solid State Communications, Vol.44,No.2, pp.89-94, 1982.
Printed in Great Britain.

0038-1098/82/380089-06$03.00/0
Pergamon Press Ltd.

LATTICE MODES IN THE LINEAR CHAIN COMPOUND $ZrTe_5$

A. Zwick, G. Landa, R. Carles and M.A. Renucci

Laboratoire de Physique des Solides, Associé au C.N.R.S., Université Paul Sabatier
118, Route de Narbonne, 31062 Toulouse Cédex, France

and

A. Kjekshus

Kjemisk Institutt, Universitetet i Oslo
Blindern, Oslo 3, Norway

(Received 13 April 1982 by M. Balkanski)

We report Raman scattering experiments on the linear chain compound $ZrTe_5$. Room and low temperature measurements rule out the existence of a structural phase transition, suggested by the resisitive anomaly near 150 K. The eight $\vec{k} = \vec{0}$ vibrationnal modes allowed by the scattering geometry are observed and their symmetries determined from polarized spectra. Some of the modes are identified on the basis of symmetry properties and (or) in comparison with the Raman spectra of the related compound $ZrTe_3$. Moreover, this comparison indicates surprisingly similar strengths for atomic interactions in $ZrTe_3$ and $ZrTe_5$.

Introduction

$ZrTe_5$ crystallizes in a chain structure [1] closely related to that of the transition-metal trichalcogenides. In some of these low dimensional compounds, such as $NbSe_3$, a particular form of the Fermi surface produces electronic instabilities which drive structural phase transitions [2,3]. This explains the recent attention devoted to the pentatellurides $ZrTe_5$ and $HfTe_5$ [4] and the subsequent investigation of their structural and transport properties by means of various techniques. In spite of a resistive anomaly [5] observed near 150 K, the other measurements [4] ruled out the possibility of an electronically-driven phase transition similar to that reported in $NbSe_3$.

In the present paper, we report the results of room and low temperature Raman scattering experiments on crystalline $ZrTe_5$. The crystal structure is described in Sec. 2. The experimental details are given in Sec. 3. Following the factor group analysis of the crystal and chain $\vec{k} = \vec{0}$ vibrationnal modes, the experimentally observed spectra are presented and discussed in Sec. 4.

2. Crystal Structure

$ZrTe_5$ was shown to be isostructural with $HfTe_5$, the crystal structure of which has been determined by the X-ray work of Furuseth et al.[1] $ZrTe_5$ crystallizes in the Cmcm (D_{2h}^{17}) space group. The conventional non-primitive unit cell contains four formula units and has the dimensions a = 3.9876 Å, b = 14.502 Å and c = 13.727 Å.

$ZrTe_5$ possesses an interesting structure with both layer and chain features that are responsible for the easy (010) cleavage and the fibrous looking of the crystals. Fig. 1(a) shows projections of the structure into different crystallographic planes, and displays the 12-atom primitive unit cell, with two chains passing through. One can build up the infinite atomic chains parallel to the a axis by stacking together distorted bicapped trigonal prisms of tellurium with the zirconium atoms located in the centre. The chains are linked by Te-Te bonds so as to form layers approximately parallel to the (010) plane. The layers are held together by weak Van der Waals-type forces.

This structure is closely related to that of $ZrTe_3$ [6] and other IV_b transition-metal trichalcogenides. The main difference, which accounts for the difference in composition, lies in the linkage between the basic coordination units [see fig. 1(b)].

3. Experiment

The samples studied in this work were single crystals of $ZrTe_5$, with typical dimensions $6 \times 0,2 \times 0,4$ mm^3. The Raman measurements were taken on freshly cleaved (010) surfaces in order to avoid scattering from Te, left behind by surface oxidation. The prepared samples were immediately immersed in the exchange gaz of an *Oxford CF 204* cryostat for room and low temperature experiments.

The Raman spectra of $ZrTe_5$, excited with the 5145 Å and 5309 Å lines of *Spectra Physics* argon and krypton ion lasers, were measured in the backscattering geometry. The laser beam was focused onto the surface sample at nearly normal incidence. The scattered light was collected along the crystal b axis direction and analyzed in a *T800 Coderg* triple monochromator, in conjunction with standard photoncounting electronics.

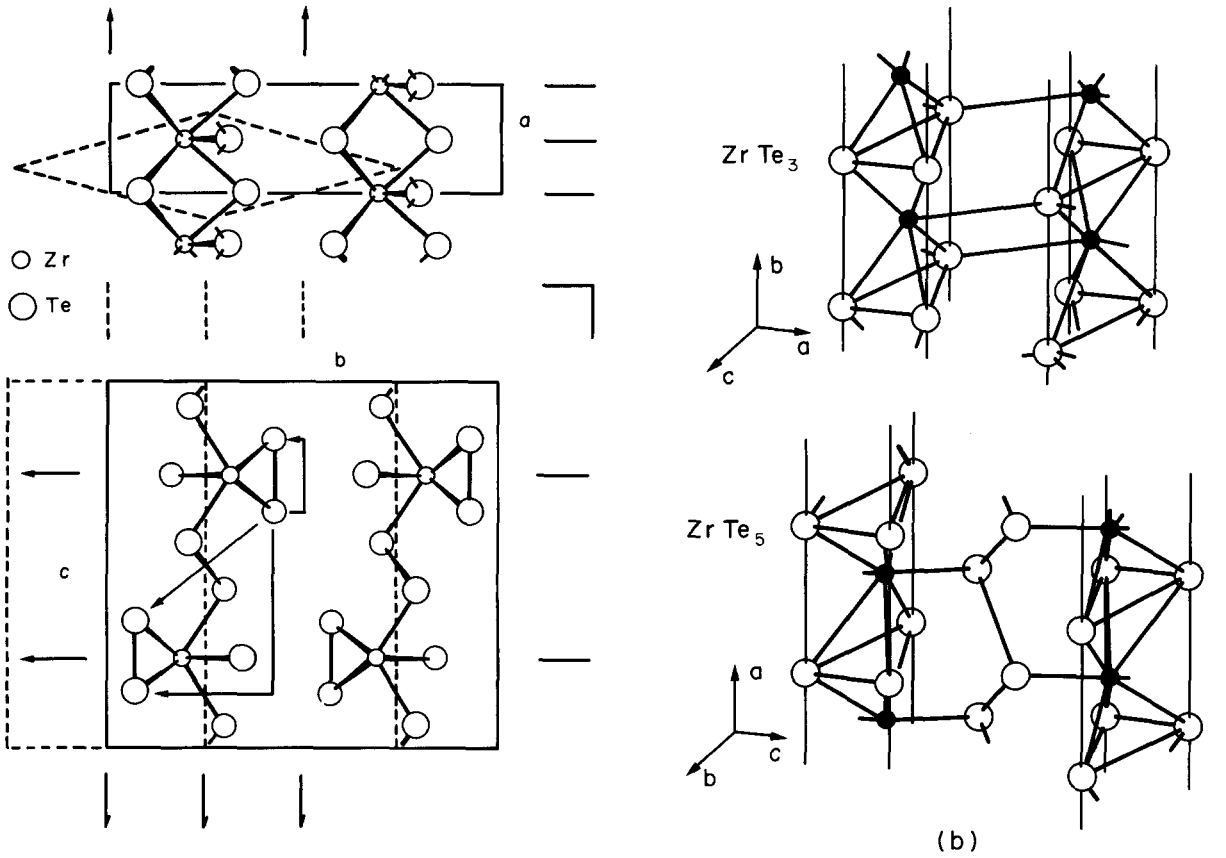

Fig.1. Structure of $ZrTe_5$ type crystals
(a) Projections in the (001) and (100) planes. The primitive unit cell is shown on the top diagram. The crystal-symmetry elements are indicated on both diagrams.
(b) Interchain linkage in $ZrTe_5$, compared to that in $ZrTe_3$.
The principal axes X, Y, Z are chosen to coïncide with the crystallographic axes a, b, c.

4. Results and Discussion

4.1. Factor group analysis

The crystal factor-group contains the eight representative symmetry elements :

1 : the identy,

2_a, 2_b : twofold axes parallel respectively to the a and b axes,

2_c : a twofold screw axis parallel to c,

$\bar{1}$: a centre of symmetry,

$\bar{2}_a$, $\bar{2}_c$: mirror planes perpendicular respectively to a and c,

$\bar{2}_b$: a glide plane perpendicular to b.

Four of these symmetry elements (the identity, the 2_b twofold axis and the $\bar{2}_a$, $\bar{2}_c$ mirror planes) are in common with the factor group of a single chain.

The symmetries of the long-wavelength phonons are determined by the representation $\Gamma_{crystal}$ of the crystal factor group generated by the displacements of the atoms in the primitive unit cell.

$\Gamma_{crystal}$ is 36 dimensional for the 12-atom primitive unit cell of $ZrTe_5$. The reduction of $\Gamma_{crystal}$ into irreducible representations of the isomorphic point group mmm (D_{2h}) is as follows :

$$\Gamma_{crystal} = 6A_g + 6B_{3g} + 2B_{2g} + 4B_{1g} + 6B_{2u} + 2A_u + 4B_{3u} + 6B_{1u}$$

Because of the inversion operation contained in the crystal factor-group, Raman and infra-red activities are mutually exclusive. The eighteen even-parity modes are optical Raman active phonons, while the eighteen odd-parity modes consist of three acoustical and fifteen optical infra-red active phonons. The $\vec{k} = \vec{0}$ modes can further be classified according to atomic displacements, parallel to the chains (or out-of-$\bar{2}_a$ mirror plane) for B_{1g}, B_{2g}, B_{3u}, A_u symmetries and perpendicular to the chains (or in $\bar{2}_a$ mirror plane) for A_g, B_{3g}, B_{2u}, B_{1u}.

Since the chains constitute well-defined

units in the crystal, it is convenient to first look at the long-wavelength modes of a single chain and then establish a compatibility relationship connecting the chain to the crystal. The chain factor-group representation Γ_{chain} generated by the displacements of atoms in the 6-atom primitive unit cell is 18 dimensional, and reducible into irreducible representations of the isomorphic point group 2mm (C_{2V}) :

$$\Gamma_{chain} : 6A_1 + 6B_1 + 2A_2 + 4B_2$$

Due to the lack of a centre of symmetry, the long-wavelength optical modes of the chain are not divided into even -and odd- symmetry types. The chains modes can be classified according to atomic displacements in -or out- of $\bar{2}_a$ mirror plane, corresponding respectively to indices 1 and 2. A and B stands for modes respectively symmetric and antisymmetric with respect to the twofold rotation. The correlation method was used to relate the irreducible representations of the zirconium and tellurium atoms site groups to those of the chain factor group. From the correlation chart presented in table I(a), we can determine which atoms move in each normal mode and wether this motion is along or perpendicular to the chain axis.

Table I(b) displays the correlation diagram relating the long-wavelength chain and crystal phonons in $ZrTe_5$. Since there are two chains per primitive unit cell correlated via an inversion centre, each chain mode splits into a g-u pair in the crystal. Furthermore, because the crystal retains all the symmetry elements of the chain, there is no mixing of the chain modes symmetries in the crystal.

In particular, the A and B symmetries do not mix, in contrast to what happens in the monoclinic structure of the IV_b metal-transition trichalcogenides. Lastly, as a result of the interchain coupling, the $A_1 + 2B_1 + B_2$ zero frequency modes of the chain divide up into four odd crystal modes (three acoustical $B_{2u} + B_{1u} + B_{3u}$ and one infra-red B_{1u}) and four low-lying even modes $A_g + 2B_{3g} + B_{1g}$. These Raman active modes are expected to be largely rigid chain motions. They can be classified in three translational modes B_{1g}, A_g, B_{3g} respectively along the a-, b- and c axes, and a librationnal mode B_{3g} about the a axis.

4.2. Experimental results and discussion

In the XYZ set of principal axes, chosen sc as to coïncide with the abc crystallographic axes of the crystal, the polarizability tensors [7] of the $\vec{k} = \vec{0}$ Raman-active modes of $ZrTe_5$ have the form :

$$A_g: \begin{bmatrix} a & . & . \\ . & b & . \\ . & . & c \end{bmatrix} \quad B_{1g}: \begin{bmatrix} . & d & . \\ d & . & . \\ . & . & . \end{bmatrix} \quad B_{2g}: \begin{bmatrix} . & . & e \\ . & . & . \\ e & . & . \end{bmatrix} \quad B_{3g}: \begin{bmatrix} . & . & . \\ . & . & f \\ . & f & . \end{bmatrix}$$

The backscattering geometry described in 3 allows the measurements of Raman tensor components XX, ZZ, XZ. Thus six A_g and two B_{2g} modes should be experimentally observed among the eighteen modes theoretically predicted.

Fig. 2 shows unanalyzed Raman spectra for two temperatures, above and below 150 K. As can be seen, eight peaks are clearly observed at room temperature. No new peak occurs at low temperature that would reveal any change of the crystallographic unit cell, such as those induced by charge density waves in many layered transition dichalcogenides [8,9].

The different components of Raman tensor allowed by the scattering geometry are shown in Fig. 3, which depicts modes polarized respectively parallel (B_{2g}) and perpendicular (A_g) to the chains. The symmetries and wavenumbers of the observed $\vec{k} = \vec{0}$ Raman active modes are given in Table II.

We shall approach the mode assignment from the analysis of the single chain vibrations, substantiated by a comparison with the Raman spectra of $ZrTe_3$. We present in Table III the list of $\vec{k} = \vec{0}$ phonons in $ZrTe_3$ and their assignment to chain modes according to the Raman works of Zwick et al.[10], and Wieting et al.[11].

As it appears from the comparison of Table III, the longwavelength phonons of $ZrTe_5$ lye very near in frequency to those of $ZrTe_3$. Beyond the close relation between the two structures, this provides evidence of similar strengths for atomic interactions in the two compounds.

Considering first in $ZrTe_5$ the two B_{2g} modes polarized along the a axis, we see from Table I(b) that they originate from A_2 chain modes. Table I(a) shows that these A_2 modes are mixtures of shearing motions of the Te_{II} and Te_{III} pairs respectively. In the crude model of bond stretching forces between nearest neighbours in the chain, the shearing motion of Te_{III} atoms does not imply any stretching of the $Zr-Te_{III}$ bonds, which are perpendicular to the chains. The interchain coupling rises this zero frequency mode until it mixes with the shearing mode of the Te_{II} pair, which depends essentially on intrachain $Zr-Te_{II}$ interaction. Assuming the same interaction between Zr and Te_{II} atoms within the chains in $ZrTe_3$ and $ZrTe_5$, we expect in $ZrTe_5$ a B_{2g} crystal doublet, very close in frequency to the B_g mode of $ZrTe_3$ originating from the shearing of the Te_{II} pair in the chain. The B_{2g} spectrum of $ZrTe_5$ (Fig.3) exhibits clearly a doublet of lines lying respectively at 74 and 89.5 cm^{-1}, close in frequency to the single B_g mode observed at 68 cm^{-1} in $ZrTe_3$. The Raman study of $ZrTe_5$ thus substantiates in turn mode assignment in $ZrTe_3$: we confidently attribute to A_2 chain mode the 68 cm^{-1} line in $ZrTe_3$, in agreement with previous assignment by Wieting and coworkers [11] based on the line intensity.

Looking now at the six A_g modes of $ZrTe_5$, we refer back to Table I(b) and conclude that they all proceed from A_1 chain modes. According to theoretical expectations, we assign the lowest lying line at 39 cm^{-1} to the quasi-rigid translationnal motion of the chains along the b-axis. Its wavenumber is surprinsingly close to that of the lowest A_g mode in $ZrTe_3$ (37 cm^{-1}), which was attributed too to a translationnal chain mode of the crystal. This might prove in turn the A_1 symmetry of the 37 cm^{-1} line of $ZrTe_3$, as we proposed in earlier work [10]. The highest frequency line at 239 cm^{-1} is attributed to the stretching mode of the diatomic $(Te_{II})_2$"molecule". This mode lies at slightly higher frequency than the corresponding mode of $ZrTe_3$ (217 cm^{-1}), that would indicate stronger atomic interaction and shorter covalent bond length between the pairing Te_{II} atoms in $ZrTe_5$ than in $ZrTe_3$. As for the others A_g lines, such a qualitative discussion

Table I.
(a) Correlation chart between C_{2V} and C_S site groups of (Zr, Te_I) and (Te_{II}, Te_{III}) atoms and C_{2V} chain factor group in $ZrTe_5$.
(b) Compatibility diagram relating the chain and crystal vibrations of $ZrTe_5$.

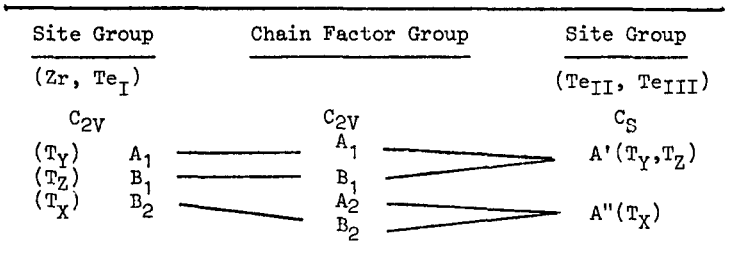

(a)

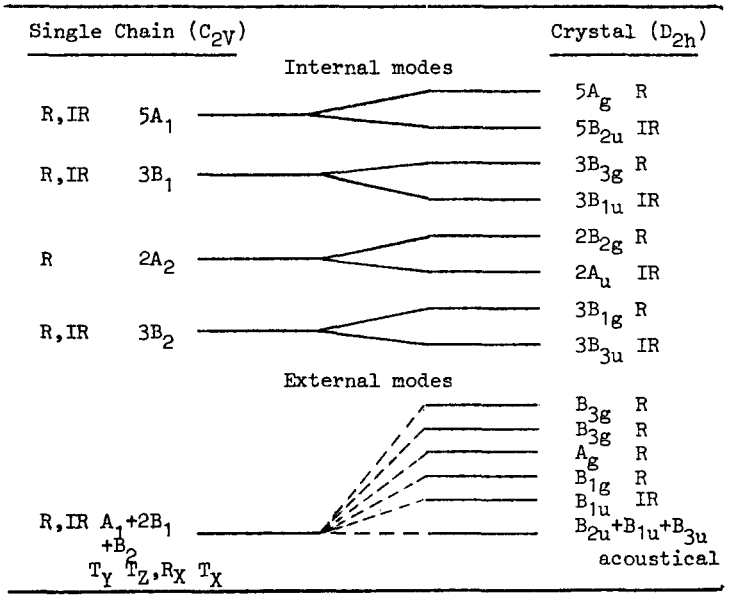

(b)

Table II. Wavenumbers and symmetries of $\vec{k} = \vec{0}$ Raman active phonons of $ZrTe_5$ at 300 K and 77 K.

Symmetry	Chain	A_1	A_2	A_2	A_1	A_1	A_1	A_1	A_1
	Crystal	A_g	B_{2g}	B_{2g}	A_g	A_g	A_g	A_g	A_g
$\nu(cm^{-1})$	300 K	39	72	86.5	116	121	147	181.5	
	77 K	40	74	89.5	117	123	152	183.5	239

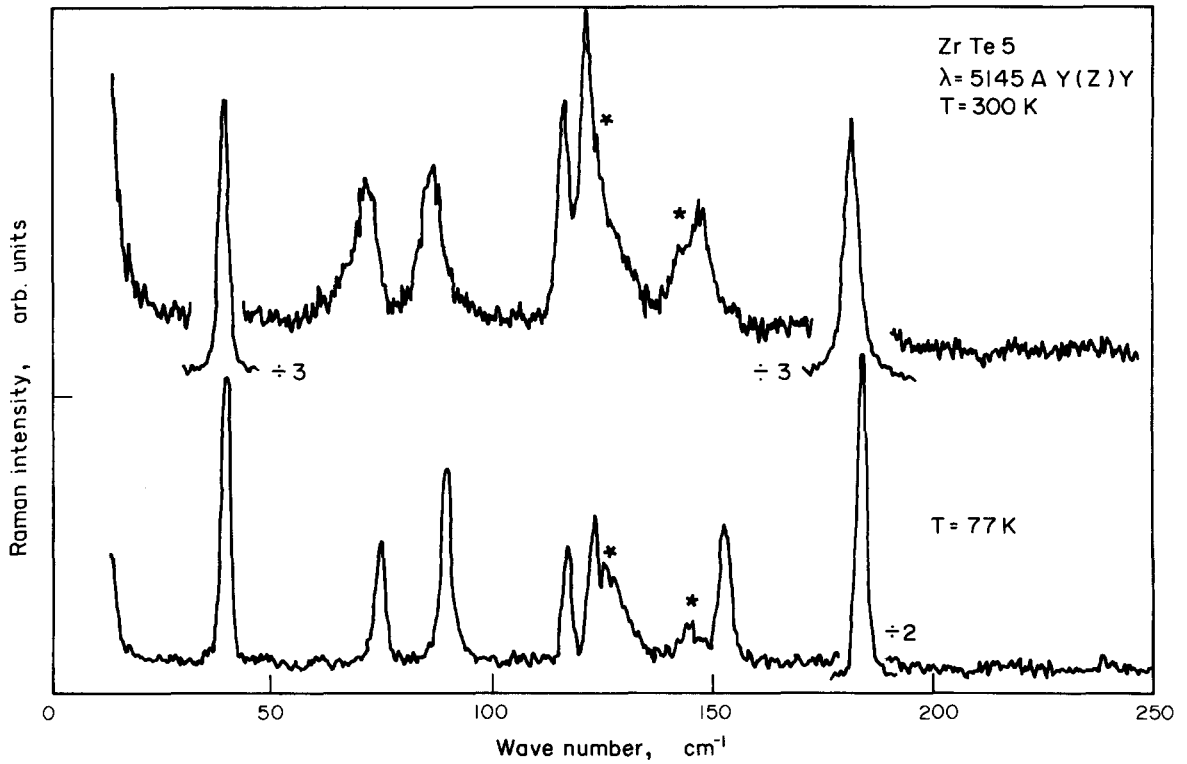

Fig.2. Unpolarized Raman spectra of $ZrTe_5$ excited with λ = 5145 Å at 300 K and 77 K. The structures marked by an asterisk are due to scattering by A_1 and E modes of crystalline Te, left behind by surface oxidation.

Table III. Wavenumbers and symmetries of $\vec{k} = \vec{0}$ Raman active phonons of $ZrTe_3$ at 300 K.

Ref. 11			Ref. 10		
Symmetry		ν (cm^{-1})	Symmetry		ν (cm^{-1})
Crystal	Chain		Crystal	Chain	
A_g	$B_1(T_X)$	11			
A_g	$B_1(R_Y)$	38	A_g	$A_1(T_Z)$	37.5
A_g	$A_1(T_Z)$	62	A_g	$B_1(T_X)$	61.5
B_g	A_2	64	B_g		66.5
A_g	B_1	86	A_g	$B_1(R_Y)$	84.5
A_g	A_1	108	A_g	A_1	111
A_g	A_1	144	A_g	A_1	143.5
A_g	A_1	216	A_g	A_1	215

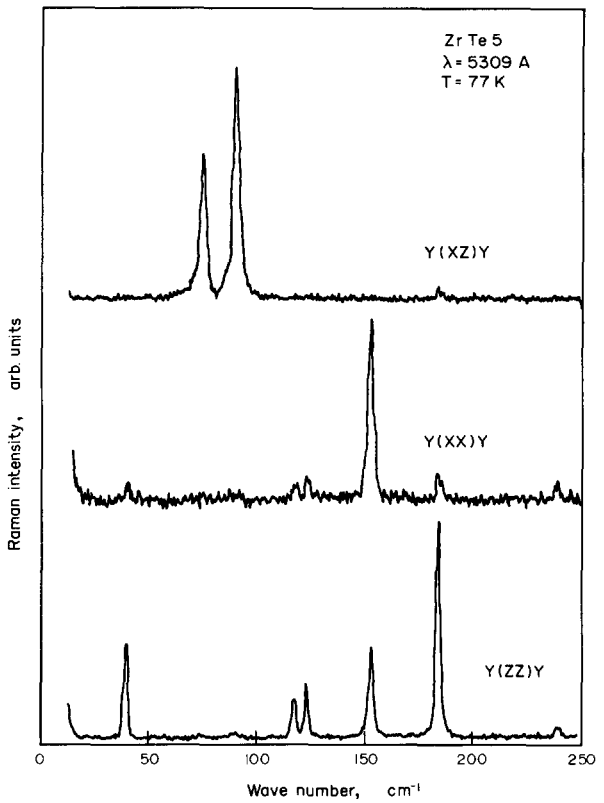

Fig.3. Polarized Raman spectra of $ZrTe_5$ excited with λ = 5309 Å at 77 K.

is not sufficient, and an interatomic-force model is needed to describe the lattice dynamics of $ZrTe_5$ and calculate the eigenvectors of the corresponding modes.

3. Conclusion

The Raman study of crystalline $ZrTe_5$ at room and liquid nitrogen temperatures rules out the possibility of an electronically driven phase transition near 150 K suggested by a resistive anomaly. All the $\vec{k} = \vec{0}$ phonons predicted by group theory analysis and allowed by the scattering geometry have been observed, and their symmetry determined by polarization measurements. An approach of the crystal lattice dynamics from the "molecular" point of view allows the identification of some crystal modes, in absence of complete calculation based on an interatomic-force model. The comparison with the Raman spectra of the closely related compound $ZrTe_3$ demonstrates that, in spite of the dissimilarity in internal architecture of the basic layers, the strengths of atomic interactions are similar in the two compounds.

References

1 S. Furuseth, L. Brattås and A. Kjekshus, *Acta Chem. Scand.* 27, 2367 (1973).
2 N.P. Ong and P. Monceau, *Phys. Rev.* B16, 3443 (1977).
3 R.M. Fleming, D.E. Moncton and D.B. McWhan, *Phys. Rev.* B15, 5560 (1976).
4 F.J. DiSalvo, R.M. Fleming and J.V. Waszczak, *Phys. Rev.* B24, 2935 (1981).
5 T.J. Wieting, D.U. Gubser, S.A. Wolf and F. Levy, *Bull. Am. Phys. Soc.* 25, 340 (1980).
6 S. Furuseth, L. Brattas and A. Kjekshus, *Acta Chem. Scand.* A29, 623 (1975).
7 R. Loudon, *Adv. Phys.* 13, 423 (1964).
8 J.R. Duffey, R.D. Kirby and R.V. Coleman, *Solid State Commun.* 20, 617 (1976).
9 J.E. Smith, J.C. Tsang and M.W. Shafer, *Solid State Commun.* 19, 283 (1976).
10 A. Zwick, M.A. Renucci and A. Kjekshus, *J. Phys. C Solid. State Phys.* 13, 5603 (1980).
11 T.J. Wieting, A. Grisel and F. Lévy, *Physica* 105B, 366 (1981).